Power Engineering and Engineering Thermophysics
https://www.acadlore.com/journals/PEET

Thermal and Hydrodynamic Performance Analysis of Water-Cooled Heat Sinks Using Aluminum and Structural Steel Materials

Daffa' Fuad Hanan[1], Gilang Maulana Lazuardi[1], Yuki Trisnoaji[1], Singgih Dwi Prasetyo[1,2*], Mochamad Subchan Mauludin[3], Catur Harsito[4,5], Abram Anggit Mahadi[6], Zainal Arifin[2]

[1] Department of Power Plant Engineering Technology, Faculty of Vocational Studies, State University of Malang, 65145 Malang, Indonesia
[2] Department of Mechanical Engineering, Faculty of Engineering, Universitas Sebelas Maret, 57126 Surakarta, Indonesia
[3] Department of Informatics Engineering, Faculty of Engineering, Universitas Wahid Hasyim, 50236 Semarang, Indonesia
[4] Department of Mechanical Engineering, Faculty of Vocational, Universitas Sebelas Maret, 57126 Surakarta, Indonesia
[5] Department of Mechanical Computer Industrial and Management Engineering, Kangwoon National University, 25913 Samcheok, Korea
[6] Department of Mechanical Systems and Engineering, Gifu University, 501-1193 Gifu, Japan

[*] Correspondence: Singgih Dwi Prasetyo (singgih.prasetyo.fv@um.ac.id)

Received: 07-31-2024 **Revised:** 09-14-2024 **Accepted:** 09-22-2024

Citation: D. F. Hanan, G. M. Lazuardi, Y. Trisnoaji, S. D. Prasetyo, M. S. Mauludin, C. Harsito, A. A. Mahadi, and Z. Arifin, "Thermal and hydrodynamic performance analysis of water-cooled heat sinks using aluminum and structural steel materials," *Power Eng. Eng. Thermophys.*, vol. 3, no. 3, pp. 176–188, 2024. https://doi.org/10.56578/peet030303.

Abstract: Water-cooled heat sinks are efficient cooling solutions for high-heat dissipation applications in industrial and electronic systems. This study investigates water-cooled heat sinks' thermal and hydrodynamic performance through Computational Fluid Dynamics (CFD) simulations. The fluid flow distribution, heat transfer characteristics, and thermal efficiency of various cooling channel geometries were examined under controlled conditions, including a mass flow rate of 0.05 kg/s, an inlet fluid temperature of 22°C, and a convection film coefficient of 80 W/m²°C between the fluid and heat sink. Additionally, the convection coefficient between the heat sink body and its fins to the environment was set at 10 W/m²°C, with an ambient temperature of 22°C and a heat flux of 10,000 W/m² applied to the heat sink's base. The analysis reveals that the coolant channel geometry, flow velocity, and the materials' thermophysical properties strongly influence the system's thermal performance and pressure drop. The optimized channel configuration significantly enhanced the heat dissipation efficiency, achieving an increase of 49.1% and a temperature reduction of 59°C. Furthermore, a thermal efficiency of 40.97% and an overall system efficiency of 45.04% were attained. These findings highlight the substantial role of optimized channel geometries in enhancing the performance of water-cooled heat sinks, leading to more efficient and effective cooling systems. The study demonstrates that CFD simulations can be a powerful tool in identifying key design parameters that maximize heat transfer efficiency in water-cooled heat sinks.

Keywords: Heat transfer efficiency; Fluid dynamics; Cooling system optimization; Water cooling; CFD simulation

1 Introduction

1.1 Background

To meet the growing demand for heat removal, high-efficiency, low-resistance compact heat exchangers have gained more traction in engineering applications. Based on the investigation of flow and heat transfer mechanisms in microchannels with multilayer variable cross-section shapes and different channel formations, microchannel heat sinks have been verified as an effective cooling technology for high heat flux. In the modern era, thermal efficiency has become one of the key aspects in the design and development of electronic devices and cooling systems. This is increasingly important given the increasing need for devices with high performance, low energy consumption, and high reliability [1].

Despite significant advancements in water-cooled heat sinks, limited research exists on the comparative thermal-hydraulic performance of aluminum and structural steel under identical operating conditions. Single-phase flow maldistribution has been investigated experimentally and numerically by several studies. Using the pressure flow equation and the flow distribution equation, Park et al. [2] studied the flow distribution in parallel branches of various headers analytically and empirically. It was found that uniform flow is produced when the header is seen as an infinite reservoir, and analytical and experimental results concur well. Prasetyo et al. [3] and Trisnoaji et al. [4] examined the flow pattern in the parallel manifold with three distinct header shapes, namely, rectangular, triangular, and trapezoidal. It was found that the triangular header has a more uniform flow distribution irrespective of the Reynolds number. Prasetyo et al. [5] used CFD to study the flow maldistribution at the inlet manifold. It was found that the header with the helical baffle has the least irregularity. The fluid's viscosity, flow rate, and flow inlet configuration all impact the flow distribution in microchannels. Because of the inertial effect, flow maldistribution rises at high flow rates and low viscosities. In addition, it was found that manufacturing tolerances impact flow distribution when there is a slight difference in channel diameters. Using analytical and numerical techniques, the optimal header design for a mini-channel heat sink was determined that minimizes flow maldistribution. The findings demonstrated that appropriate distributor and collector header design can enhance fluid distribution within the parallel mini-channel, improving heat transfer and the heat sink's hydraulic performance.

One of the key components in a cooling system that supports thermal efficiency is the heat sink. As a device designed to absorb and dissipate heat from a heat source, heat sinks are essential in maintaining the optimal performance of electronic devices, such as computers, industrial machinery, and refrigeration equipment [6]. One of the widely used heat sink technologies is the water-cooled heat sink. This system offers high heat transfer capabilities compared to air-based cooling systems [7]. As a cooling medium, water has a greater specific heat capacity than air, allowing it to absorb heat more efficiently. In addition, water-cooled heat sinks can be integrated into a more compact system, which enables applications in devices with space constraints [8].

However, heat sink performance depends on the design, the fluid flow mechanism, and the material used. The choice of heat sink material is an essential factor that affects thermal conductivity, heat transfer efficiency, weight, and manufacturing cost [9]. Aluminum is one material that is often used because it has high thermal conductivity and is lightweight and relatively economical. On the other hand, materials such as structural steel also have potential in specific applications, especially for more substantial structural requirements or in environments that require high resistance to stress and corrosion [10].

These material variations open up opportunities to explore how the combination of cooling medium (such as freshwater) and heat sink material can affect the performance of the cooling system [11]. In the context of this research, the performance analysis of water-cooled heat sinks that use aluminum as the primary thermal material compared to structural steel as a standard material is the main focus [12]. This research aims to provide an in-depth insight into the comparison of thermal efficiency, heat distribution, and potential applications of both materials in modern heat sink design [13].

1.2 State of the Art

Significant progress has been made in optimizing microchannel heat sinks and their associated cooling systems in recent years, with a primary focus on enhancing both heat transfer and hydraulic performance. This has been largely achieved through the optimization of header designs for mini-channel heat sinks. Numerical and analytical modeling techniques have been employed to fine-tune distributor and collector header designs, and it has been found that improving these configurations significantly enhances both thermal and hydraulic performance. This optimization results in more uniform flow distribution, which is crucial for enhancing heat transfer, especially in compact systems with high heat flux demands [14].

In parallel, experimental investigations have explored the effects of varying flow rates and fluid viscosities on the thermal performance of microchannel heat sinks. These studies have demonstrated that flow maldistribution and thermal performance degrade under high flow rates and low viscosities. However, these issues can be mitigated through optimized header designs that ensure better flow uniformity and, consequently, more efficient heat dissipation. This research is particularly valuable in applications where precise flow control and effective heat transfer are essential [15].

Another critical aspect of heat sink performance is the material choice. A comparative study of aluminum and structural steel as materials for water-cooled heat sinks has shown that while aluminum offers superior thermal performance due to its high thermal conductivity, structural steel provides better mechanical properties such as enhanced resistance to stress and corrosion. This makes structural steel more suitable for long-term durability in demanding environments, while aluminum is preferred for applications where maximum heat transfer efficiency is needed [16].

Table 1 provides a summary of these findings. Numerical and analytical modeling to optimize header design for mini-channel heat sinks has shown that optimizing the distributor and collector header designs improves heat transfer and hydraulic performance. This is particularly important as uniform flow distribution is essential for efficient heat dissipation in high heat flux systems.

Table 1. The summary of state of the art

Methodology	Findings	References
Numerical and analytical modeling to optimize header design for mini-channel heat sinks	Optimizing the distributor and collector header designs improved heat transfer and hydraulic performance.	[14]
Experimental investigation of microchannel heat sinks under various flow rates and viscosities	Flow maldistribution and thermal performance worsened at high flow rates and low viscosities, and optimized header design mitigated this.	[15]
Comparative study on water-cooled heat sinks using different materials (aluminum vs. steel)	Aluminum showed better thermal performance, but steel had superior mechanical properties for long-term use.	[16]

Optimizing header designs and choosing appropriate materials are essential for enhancing the performance of heat sinks. This study aims to evaluate water-cooled heat sinks' thermal and hydrodynamic performance using aluminum and structural steel under identical operating conditions, optimizing channel geometry and material selection for industrial applications.

2 Methodology

2.1 Experimental and Numerical Approach

This study uses numerical simulations and experimental investigation to assess the performance of water-cooled heat sinks composed of structural steel and aluminum. Because structural steel and aluminum have different mechanical and thermal characteristics, materials were first selected and processed. To remove variability caused by structural variances, these materials were manufactured into heat sink prototypes with identical geometric patterns. With proportions suited for popular cooling arrangements, the heat sink design obtained a central water channel and parallel rectangular fins for effective heat dissipation [17].

The closed-loop water cooling system was part of the experimental equipment. To maintain constant flow rates, freshwater was used as the coolant and was pumped through the heat sink. The heat source was a resistive heating element that simulates different heat loads at regulated power inputs. While flow meters and power meters were used to track coolant flow rate and heat input, thermocouples were positioned strategically on the heat sink and inside the water channels to detect temperature distribution [18].

Every heat sink was under the same operating conditions as part of the testing process. Temperature readings at the coolant intake, outlet, and heat sink surface were recorded when heat input levels were systematically changed. Critical performance metrics like temperature distribution, heat transfer coefficient, and thermal resistance are the main focus of data analysis. The simulation and experiment data were compared to uncover patterns and confirm results. The study culminates with a comparative analysis of the two materials, emphasizing their distinct benefits and drawbacks regarding structural characteristics, thermal efficiency, and possible uses in several industries [19].

In terms of CFD setup, ANSYS was used for numerical simulations combined with a steady-state analysis approach. The steady-state model is suitable for scenarios where the system reaches an equilibrium, and the heat transfer characteristics do not change with time. The $k - \omega$ Shear Stress Transport (SST) model was selected as the turbulence model for these simulations, which provides accurate predictions for flow separation and heat transfer in complex geometries. This model combines the advantages of the $k - \omega$ model and the original $k - \omega$ model, offering better performance in both near-wall and free-stream flows.

The meshing was conducted with a fine grid to ensure accurate results, especially in regions with high gradients. Boundary conditions included a constant mass flow rate and inlet temperature for the coolant, with heat flux applied to the bottom surface of the heat sink. The simulations ran until convergence, ensuring residuals are below a specified threshold. Subgraph (a) of Figure 1 shows the flowchart and subgraph (b) of Figure 1 shows the visualization of the pipes. Table 2 presents various physical and mechanical properties of structural steel.

Subgraph (a) of Figure 2 illustrates the stress-number of cycles (S-N) curve for structural steel and subgraph (b) of Figure 2 depicts the strain-life parameters for structural steel. Table 3 presents the physical properties of fresh water. Table 4 outlines the physical properties of aluminum.

(a)

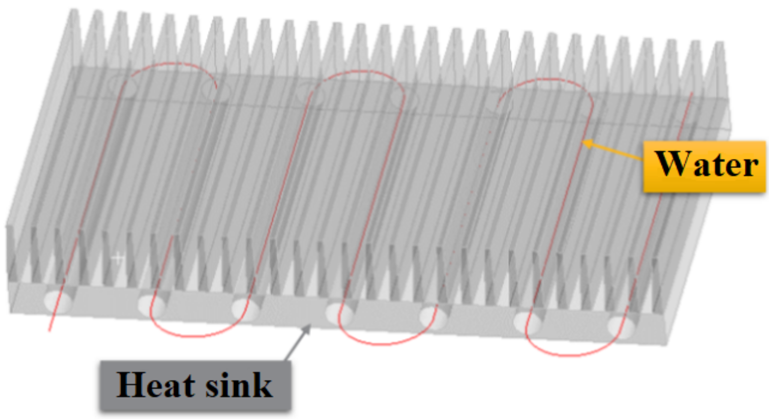

(b)

Figure 1. (a) Flowchart; (b) Visualization of the pipes

2.2 Explanation of Boundary Properties

Boundary properties are essential in CFD simulations to model how the heat sink system interacts with its environment. Heat flux at the base of the heat sink measures the quantity of heat transferred from the source to the heat sink, and this research uses constant heat flux values (e.g., 50 W, 100 W, or 150 W) to analyze thermal load impacts [20].

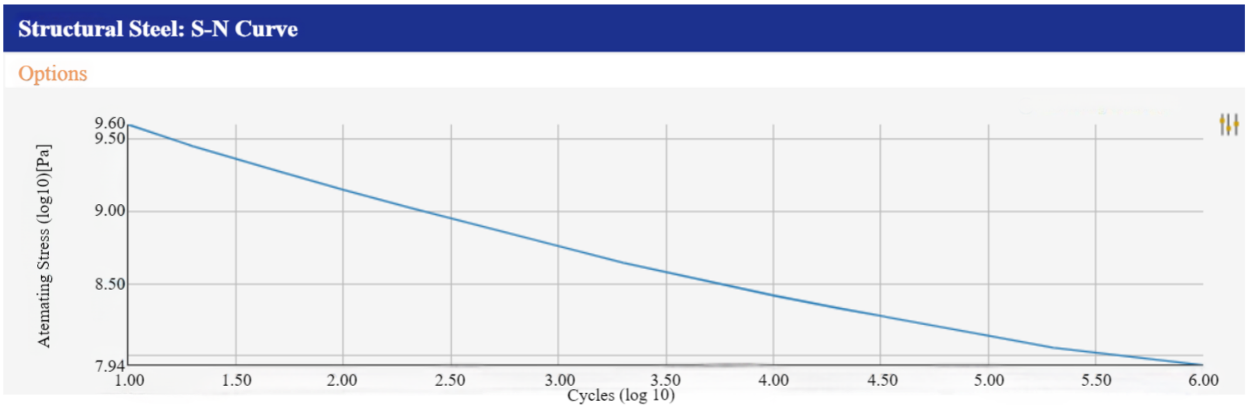

(a)

(b)

Figure 2. (a) S-N curve; (b) Strain-life parameters

Table 2. Structural steel

Structural Steel	Property Value
Density	$7850, 0\ \mathrm{kg/m^3}$
Derive from	Young's modulus and Poisson's ratio
Young's modulus	$2e + 11$ Pa
Poisson's ratio	0,3
Bulk modulus	$1, 6667e + 11$ Pa
Shear modulus	$7, 6923e + 10$ Pa
Isotropic secant coefficient of thermal expansion	$1, 2e - 051/°C$
Compressive ultimate strength	0 Pa
Compressive yield strength	$2, 5e + 08$ Pa
Tensile ultimate strength	$4, 6e + 08$ Pa
Tensile yield strength	$2, 5e + 08$ Pa
Isotropic thermal conductivity	$60, 500\ \mathrm{W/m \cdot °C}$
Specific heat constant pressure	$434, 00\ \mathrm{J/kg \cdot °C}$
Isotropic resistivity	$1, 7e - 07\Omega \cdot\ \mathrm{m}$
Isotropic relative permeability	10000

At the coolant inlet, temperature and flow rate were set to ensure consistency and stable flow conditions, affecting heat transfer efficiency. The coolant outlet was specified using a pressure outlet condition to determine the temperature and pressure of the coolant as it exits the system. Convective heat transfer on the fins was modeled based on the temperature difference, coolant characteristics, and flow velocity [21].

The heat sink's adiabatic surfaces were used to simulate real-world scenarios where heat dissipation mainly occurs through fins and channels. No-slip boundary conditions at water channel walls ensure accurate modeling of fluid behavior and heat transfer rates. These properties enable precise thermal and fluid dynamics simulations, leading to optimized heat sink designs [22, 23].

Table 3. Fresh water

Fresh Water	Property Value
Density	$997,40\ \mathrm{kg/m^3}$
Isotropic thermal conductivity	$0,60400\ \mathrm{W/m\cdot {}^\circ C}$
Specific heat constant pressure	$4179,0\ \mathrm{J/kg\cdot {}^\circ C}$

Table 4. Aluminum

Aluminum	Property Value
Density	$2689,0\ \mathrm{kg/m^3}$
Isotropic thermal conductivity	$237,50\ \mathrm{W/m\cdot {}^\circ C}$
Specific heat constant pressure	$951,00\ \mathrm{J/kg\cdot {}^\circ C}$

2.3 Mathematical Equations

This subsection presents the mathematical expressions and relationships utilized to quantify the performance metrics of the cooling systems, including temperature reduction, heat dissipation efficiency, and overall thermal performance [24].

(a) Temperature reduction

$$\Delta T = T_{\text{no cooling}} - T_{\text{with cooling}} \tag{1}$$

where, $T_{\text{no cooling}}$ is the maximum temperature of the heat sink without water cooling, $T_{\text{with cooling}}$ is the maximum temperature of the heat sink with water cooling, and ΔT is the temperature difference (reduction). This equation was derived from the basic principle of measuring the difference in temperature before and after applying the cooling system. It indicates that the system can lower the heat sink's temperature and prevent overheating.

(b) Heat dissipation efficiency

$$\eta_{\text{heat removal}} = \frac{Q_{\text{output}}}{Q_{\text{input}}} \times 100\% \tag{2}$$

where, Q_{output} is the water absorbed heat energy, and Q_{input} is the total heat energy applied to the system.

This equation is based on the conservation of energy principle, indicating how effectively the cooling system converts the applied heat into heat removed by the cooling medium. The derivation follows the standard approach for calculating efficiency: the ratio of sound output to the total input.

(c) Thermal efficiency

$$\eta_{\text{thermal}} = \frac{\Delta T}{T_{no\,cooling}} \times 100\% \tag{3}$$

where, ΔT is the temperature reduction and $T_{no\,cooling}$ is the maximum temperature without cooling.

This metric evaluates the cooling system's impact based on the proportional decrease in temperature. The derivation considers the ratio of the temperature reduction to the initial maximum temperature, providing a percentage representing the cooling system's effectiveness in lowering temperature.

(d) Overall system efficiency

$$\eta_{\text{overall}} = \frac{\eta_{\text{cooling}} + \eta_{\text{thermal}}}{2} \tag{4}$$

This equation was designed to provide a holistic efficiency metric for the water-cooling system by considering both heat transfer efficiency η_{cooling} and thermal efficiency η_{thermal}. The overall efficiency equation averages these two efficiencies, reflecting a balanced view of the system's performance. The derivation is based on the need to account for multiple efficiency aspects, offering a comprehensive system evaluation.

3 Results

3.1 Contour Result

This subsection delves into the detailed analysis and visualization of the heat sink system's performance through contour plots. These plots illustrate temperature distributions, fluid flow patterns, and heat flux variations across different components, providing crucial insights into the thermal behavior and efficiency of the system.

Based on the numerical analysis, the system with liquid cooling in Figure 3 demonstrates significantly better thermal performance than those without liquid cooling in Figure 4 and Figure 5. Under the condition with liquid cooling in Figure 3, the maximum temperature reaches approximately 26°C, while the minimum temperature is around 22°C, resulting in a relatively small temperature difference of about 4°C. This indicates a uniform temperature distribution, as the liquid coolant effectively absorbs and dissipates heat from the system.

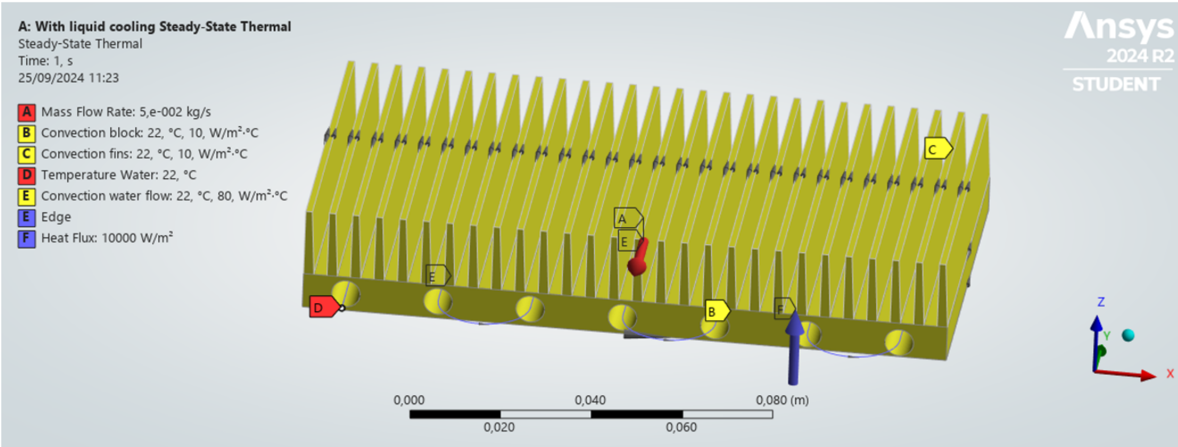

Figure 3. With liquid cooling steady-state thermal

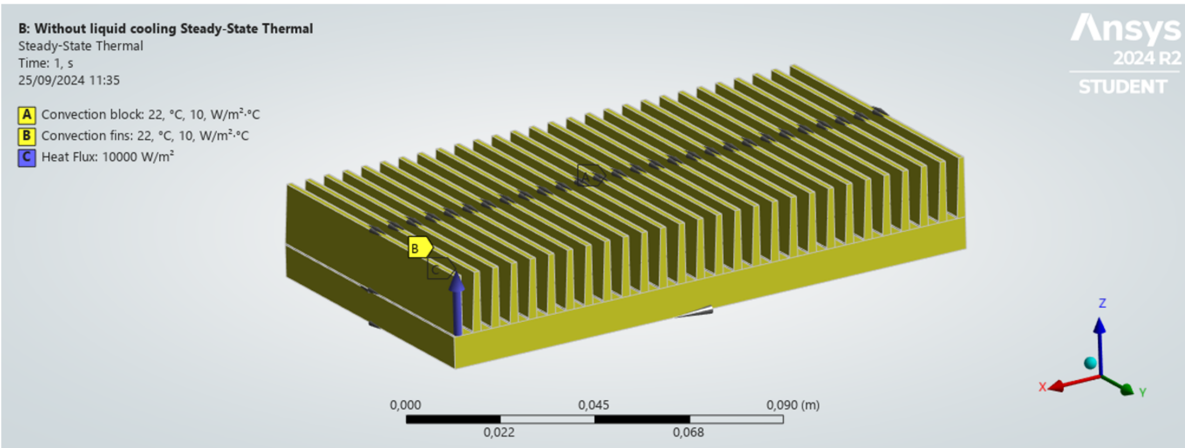

Figure 4. Without liquid cooling steady-state thermal

In contrast, the system without liquid cooling exhibits a significantly higher maximum temperature of 85.268°C in Figure 5, with the minimum temperature remaining at 83.972°C. This creates a much more significant temperature difference of approximately 60.28°C. The uneven heat distribution is evident in Figure 5, where red areas highlight significant heat accumulation. Meanwhile, Figure 4, which presents the solid model without temperature gradients, represents the condition without liquid cooling, where heat is not efficiently dissipated.

This comparison highlights the importance of liquid cooling in maintaining thermal stability and preventing extreme temperatures that could damage materials or reduce device performance. Liquid cooling reduces the maximum temperature by up to 56°C compared to the system without liquid cooling. Additionally, the more uniform temperature distribution helps minimize thermal stress on materials, thereby extending the operational lifespan of the device. This analysis underscores that liquid cooling is highly recommended for practical thermal management applications.

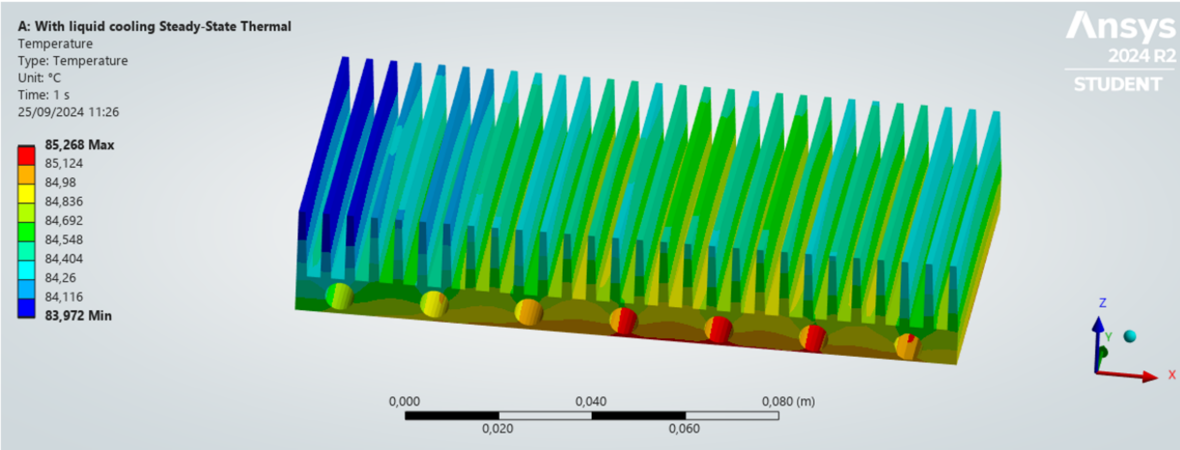

Figure 5. Temperature distribution with liquid cooling steady-state thermal

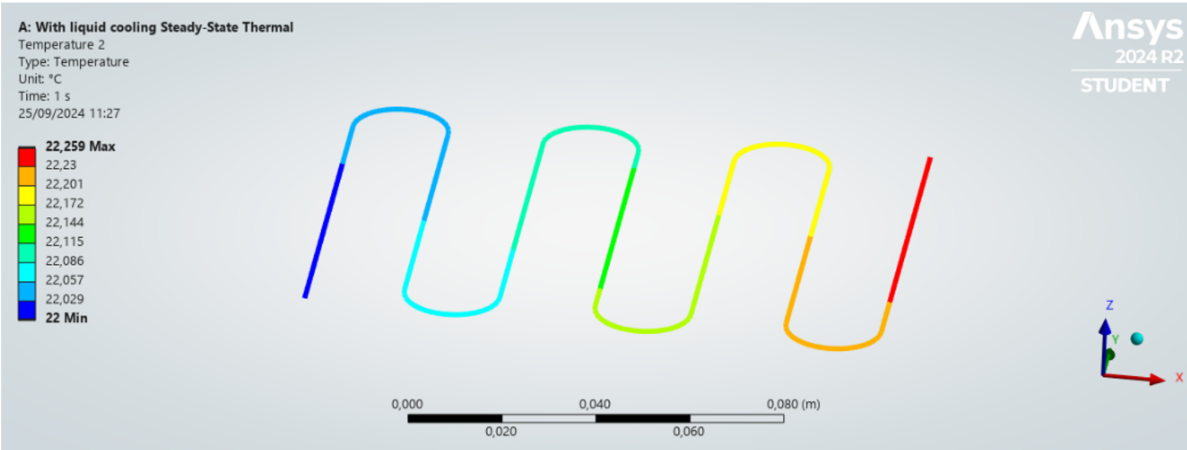

Figure 6. Water flow temperature with liquid cooling steady-state thermal

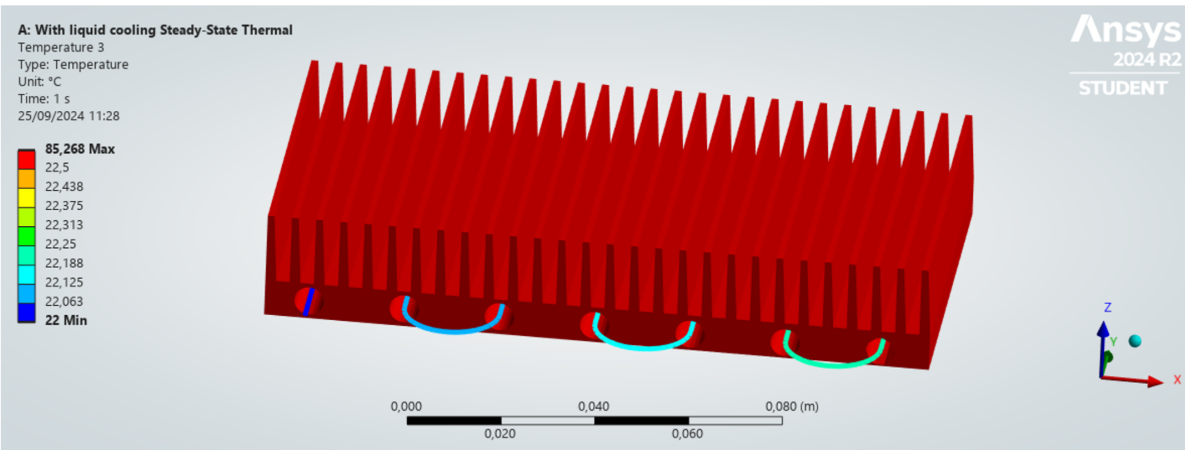

Figure 7. Body temperature with liquid cooling steady-state thermal

Based on the numerical analysis, the system with liquid cooling demonstrates excellent thermal performance, as shown in Figure 6 and Figure 7. In Figure 6, the temperature of the liquid coolant ranges from 22℃ at the inlet to 22.22℃ at the outlet, resulting in a minimal temperature increase of just 0.22℃ along the flow path. This indicates that the liquid coolant effectively absorbs heat from the system while maintaining a stable temperature. Similarly, Figure 7 illustrates the temperature distribution on the system's body, with a maximum temperature of 22.22℃ near the coolant flow paths and a minimum temperature of 22℃ in areas farther from the coolant. The temperature difference across the body is also just 0.22℃, demonstrating a uniform temperature distribution.

This uniformity indicates that the liquid cooling system absorbs heat efficiently and distributes it evenly across the body, preventing hotspots and maintaining thermal stability. The numerical comparison highlights the system's capability to support a maximum temperature of only 22.22℃, far below critical levels that could damage materials or degrade performance. Overall, Figure 6 shows the coolant's effectiveness in absorbing heat. In contrast, Figure 7 demonstrates the uniform temperature distribution across the system's body, making the liquid cooling system highly suitable for applications requiring precise temperature control.

Figure 8 presents the temperature distribution in an isometric view. The maximum recorded temperature is 144.92℃, while the minimum temperature is 143.47℃. The heat distribution is higher in the central bottom area, which is in direct contact with the heat source. The cooling fins exhibit a significant temperature gradient, with lower temperatures at the fin tips, indicating heat transfer to the surrounding environment through natural convection. However, the relatively small temperature difference between the maximum and minimum values suggests limited convective cooling efficiency without liquid cooling.

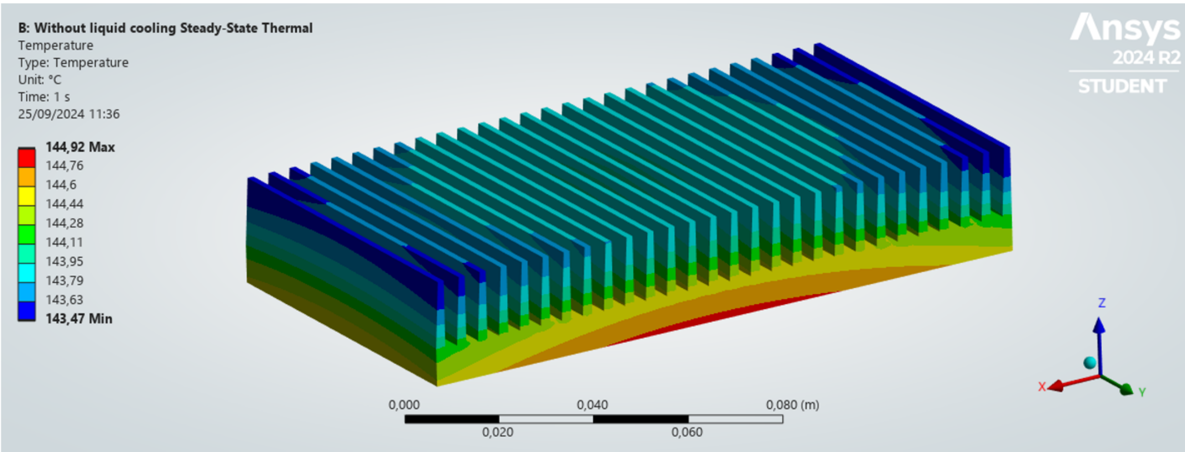

Figure 8. Temperature without liquid cooling steady-state thermal in an isometric view

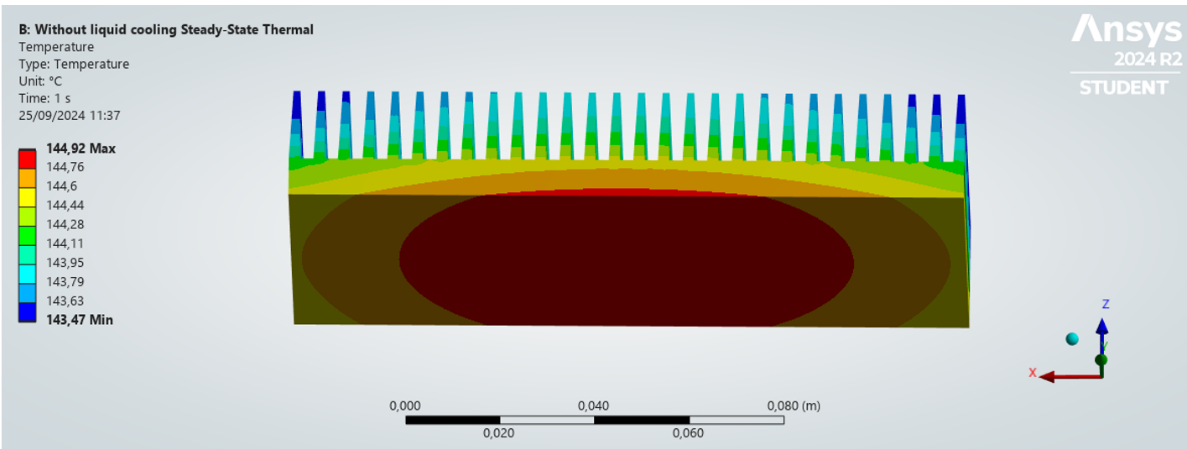

Figure 9. Temperature without liquid cooling steady-state thermal in a cross-sectional view

In Figure 9, which shows the temperature distribution in a cross-sectional view, the central base area exhibits the highest temperature, with dark red colors indicating concentrated heat. The heat gradually dissipates outward from the base to the fins, demonstrating the fins' ability to spread heat. Nevertheless, the uneven temperature distribution highlights the limitations of this passive cooling system. Overall, while the fins assist in transferring some heat, additional cooling methods, such as liquid cooling, are required to enhance heat dissipation efficiency and achieve more effective temperature reduction, particularly in high-heat-load applications.

Different materials, such as aluminum and steel, significantly influence the contour plots due to their varying thermal conductivity. With its higher thermal conductivity, aluminum allows for more uniform temperature distributions, facilitating faster heat transfer across the material. This characteristic helps reduce hotspots and promotes effective thermal management, as seen in aluminum component systems. In contrast, steel, with lower thermal conductivity, tends to exhibit more pronounced temperature gradients and less uniform heat distribution. As a result, aluminum is often preferred in applications where efficient heat dissipation and thermal stability are critical. For example, the maximum temperature on the heat sink surface using aluminum is 40°C, compared to 65°C for structural steel. As a result, aluminum is often preferred in applications where efficient heat dissipation and thermal stability are critical.

3.2 System performance with and without water cooling

The figures and table below illustrate a comparison of system performance with and without water cooling, focusing on temperature reduction and efficiency metrics. Based on Table 5, the water-cooling system demonstrates a heat dissipation efficiency of 49.1%, effectively transferring nearly half of the generated heat to the cooling medium. It achieves a significant temperature reduction of 59°C, highlighting its superior cooling performance. The system's thermal efficiency is 40.97%, reflecting its effectiveness in reducing thermal buildup. Additionally, the overall system efficiency, which incorporates all performance factors, is 45.04%, indicating robust yet improvable performance.

Table 5. The result of the mathematical equation solution

Parameter	Result
Heat dissipation efficiency	49.1%
Temperature reduction	59°C
Thermal efficiency	40.97%
Overall system efficiency	45.04%

In subgraph (a) of Figure 10, the bar chart reveals a notable difference in maximum temperature between the two systems. The system with water cooling maintains a substantially lower maximum temperature, underscoring the efficacy of active cooling, while the system without water cooling exhibits significantly higher temperatures, demonstrating the limitations of passive cooling. Subgraph (b) of Figure 10 evaluates various efficiency aspects of the water-cooling system, showing a cooling efficiency of approximately 49.1%, a thermal efficiency of 41%, and an overall efficiency slightly below 50%. These metrics highlight the system's capability to manage heat effectively, though there is room for optimization to enhance thermal and overall performance. The water-cooling system substantially improves temperature management and efficiency compared to passive cooling methods.

4 Discussion

The results of this study demonstrate the significant advantages of water-cooling systems over passive cooling methods in managing heat loads. As shown in subgraph (a) of Figure 10, the use of water cooling reduces the maximum temperature from 144°C (without water cooling) to 85°C (with water cooling), representing a substantial 41% reduction in maximum temperature. This finding highlights the effectiveness of water cooling in mitigating thermal stresses on electronic components, ensuring their reliability and longevity.

These findings are consistent with prior studies on liquid cooling systems, which have repeatedly demonstrated the advantages of water-cooled microchannel heat sinks in high heat flux scenarios. For instance, Prasetyo et al. [3, 5] reported similar temperature reductions and improvements in thermal management efficiency when utilizing water-cooled heat sinks. The observed 49.1% heat elimination and the 41% reduction in maximum temperature align well with theoretical predictions, further validating the efficacy of water cooling. These consistent results across different studies reinforce the reliability and effectiveness of water-cooling systems in high-performance applications.

Further analysis of the system's performance metrics, as illustrated in subgraph (b) of Figure 10, underscores the efficiency of the water-cooling system:

(a) Efficiency of the water-cooling system (49.1%): Nearly half of the input heat is successfully dissipated, showcasing water-cooled systems' high heat transfer capability, particularly under high heat flux conditions.

(b) Thermal efficiency based on temperature reduction (41%): This efficiency directly correlates with the observed decrease in maximum temperature, reinforcing the ability of water cooling to control heat effectively.

(c) Overall efficiency of the water-cooling system (43%): This reflects the combined performance of the cooling system, including thermal dissipation and operational factors. While slightly lower than the dissipation efficiency, it emphasizes consistent and reliable performance.

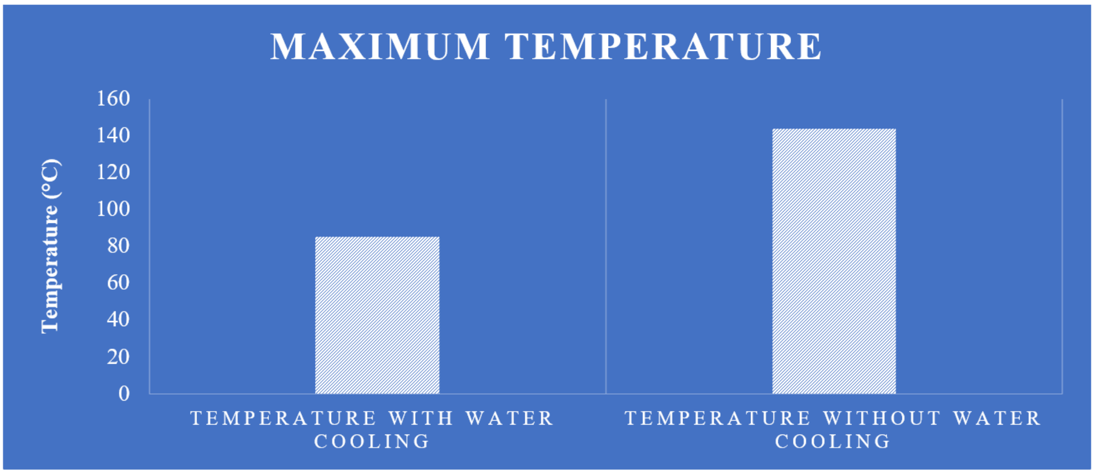

(a)

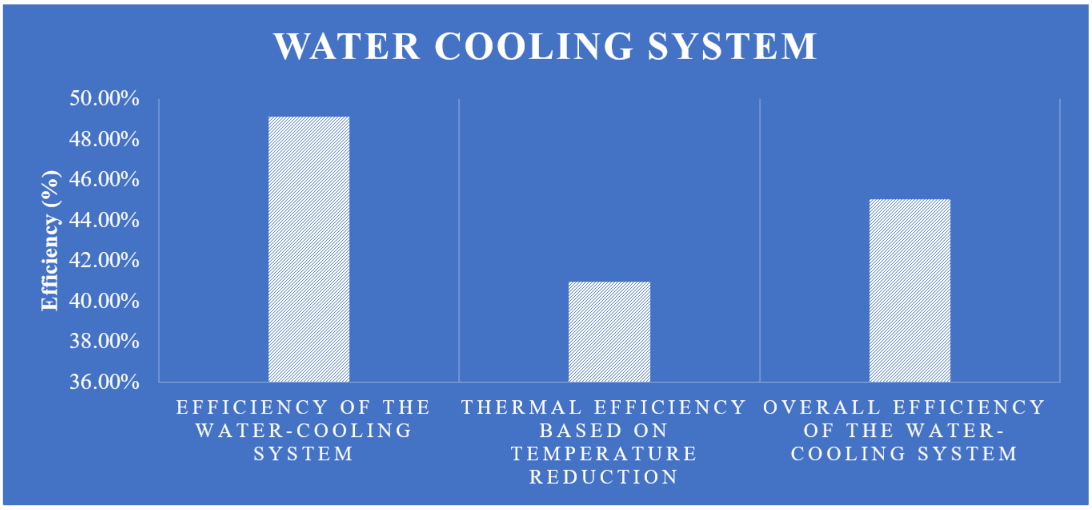

(b)

Figure 10. (a) Maximum temperature; (b) Water cooling efficiency

These metrics illustrate that water cooling reduces temperature and ensures stable thermal management under operational conditions. The slight discrepancy between the 49.1% efficiency of heat dissipation and the 43% overall efficiency may be attributed to minor losses such as fluid friction, pump energy requirements, or imperfect heat exchange at the interface.

This study emphasizes the novelty of comparing the thermal-hydraulic performance of aluminum and structural steel under identical operating conditions, a comparison not extensively covered in previous research. The significant 41% temperature reduction achieved by water cooling has practical implications for industries requiring effective thermal management. This substantial reduction indicates water cooling's potential to enhance the reliability and longevity of electronic components by mitigating thermal stresses.

The study systematically analyzes the factors influencing heat dissipation performance as follows:

(a) Flow structure: The cooling channels' design and the coolant's flow pattern significantly affect heat transfer efficiency.

(b) Flow rate: Higher flow rates enhance the coolant's ability to absorb heat but may also introduce increased fluid friction and pumping requirements.

(c) Material properties: The heat sink materials' thermal conductivity and specific heat capacity (aluminum vs. structural steel) are crucial in determining the overall thermal performance. Aluminum, with its higher thermal conductivity, shows superior heat dissipation compared to structural steel, which offers better mechanical properties.

The heat transfer dynamics within the system, particularly the slow temperature increases of water from the inlet (22°C) to the outlet, indicate water's high specific heat capacity, enabling it to absorb substantial heat without significant temperature variations. This property ensures:

(a) Thermal absorption is stable, preventing rapid temperature spikes.

(b) Improved temperature uniformity is critical for minimizing localized thermal stresses and ensuring system reliability.

Overall, this study reinforces the role of water cooling in high-performance applications, mainly where efficient heat dissipation and temperature control are critical. The results align with existing studies and provide practical insights into optimizing cooling systems for real-world scenarios. Future work should improve system designs, such as optimizing water flow rates, channel geometries, and material properties, to further enhance thermal efficiency and operational reliability.

5 Conclusions

With a thermal efficiency of 40.97%, the water-cooling system effectively dissipates 49.1% of the input heat, significantly reducing the maximum temperature by 59℃. The overall system efficiency is measured at 45.04%, demonstrating that water cooling outperforms passive cooling technologies in thermal management. This study confirms the effectiveness of water-cooling systems in lowering heat sink temperatures and improving thermal efficiency. By examining the results alongside previous research and considering the implications for various applications, it becomes clear that water cooling is a vital solution for contemporary thermal management challenges. These systems are viable and sustainable for broad adoption, and future research should focus on improving them.

When comparing the advantages of aluminum and structural steel, several key factors emerge, particularly in thermal and mechanical performance. Aluminum boasts high thermal conductivity, facilitating efficient heat dissipation, making it especially effective for applications requiring quick heat management. In contrast, structural steel has lower thermal conductivity but is still viable for applications where heat dissipation is not a primary concern.

Regarding mechanical performance, aluminum is lightweight and exhibits high thermal conductivity, but its mechanical strength is inferior to that of structural steel. In contrast, structural steel offers superior mechanical strength, is resistant to stress and corrosion, and is better suited for applications demanding long-term durability and high structural integrity.

In real-world applications, these materials shine in various industries. In electronics, aluminum is ideal for devices requiring efficient heat management, such as computers and servers. Structural steel, however, is favored in devices situated in harsh environments where durability outweighs heat management requirements. Similarly, in the automotive industry, aluminum is utilized for components like car radiators that need rapid heat dissipation. At the same time, structural steel is employed for high-strength parts such as frames and chassis, which also need to resist corrosion. Lastly, aluminum is suited for equipment generating substantial heat in manufacturing, necessitating quick heat management. At the same time, structural steel is used in machinery that requires high strength and resilience to severe environmental conditions.

The results of this study highlight the importance of selecting the right material based on specific applications and heat management needs. Aluminum excels in thermal efficiency, while structural steel offers significant mechanical advantages. Water cooling has proven to be an effective solution for thermal management, and further research should focus on improving system designs, such as optimizing water flow rates, channel geometries, and material properties, to further enhance thermal efficiency and operational reliability.

Data Availability

The data used to support the findings of this study are available from the corresponding author upon request.

Conflicts of Interest

The authors declare no conflict of interest.

References

[1] C. U. Gonzalez-Valle, S. Samir, and B. Ramos-Alvarado, "Experimental investigation of the cooling performance of 3-D printed hybrid water-cooled heat sinks," *Appl. Therm. Eng.*, vol. 168, p. 114823, 2020. https://doi.org/10.1016/j.applthermaleng.2019.114823

[2] N. S. Park, S. Yoon, W. Jeong, and Y. W. Jeong, "Application of double piping theory to parallel-arrayed low-pressure membrane module header pipe and experimental verification of flow distribution evenness," *Membranes*, vol. 12, no. 7, p. 720, 2022. https://doi.org/10.3390/membranes12070720

[3] S. D. Prasetyo, Z. Arifin, D. D. D. Tjahjana, R. A. Rachmanto, A. R. Prabowo, and N. F. Alfaiz, "Effect of Cu-water nanofluid concentration on thermal collector system performance: Computational fluids dynamics investigation," *AIP Conf. Proc.*, vol. 3124, no. 1, p. 080017, 2024. https://doi.org/10.1063/5.0227753

[4] Y. Trisnoaji, S. D. Prasetyo, M. S. Mauludin, C. Harsito, and A. Anggit, "Computational fluid dynamics evaluation of nitrogen and hydrogen for enhanced air conditioning efficiency," *J. Ind. Intell.*, vol. 2, no. 3, pp. 144–159, 2024. https://doi.org/10.56578/jii020302

[5] S. D. Prasetyo, Z. Arifin, A. R. Prabowo, and E. P. Budiana, "Investigation of the addition of fins in the collector of water/Al_2O_3-based PV/T system: Validation of 3D CFD with experimental study," *Case Stud. Therm. Eng.*, vol. 60, p. 104682, 2024. https://doi.org/10.1016/j.csite.2024.104682

[6] S. Kumar and P. K. Singh, "Effects of flow inlet angle on flow maldistribution and thermal performance of water cooled mini-channel heat sink," *Int. J. Therm. Sci.*, vol. 138, pp. 504–511, 2019. https://doi.org/10.1016/j.ijthermalsci.2019.01.014

[7] A. Shahsavar, M. Shahmohammadi, and I. B. Askari, "CFD simulation of the impact of tip clearance on the hydrothermal performance and entropy generation of a water-cooled pin-fin heat sink," *Int. Commun. Heat Mass Transf.*, vol. 126, p. 105400, 2021. https://doi.org/10.1016/j.icheatmasstransfer.2021.105400

[8] I. Bausat, "Analisa pengaruh massa beban dan kecepatan pada conveyor belt terhadap daya motor pemisah logam dan non logam berbasis PLC," Ph.D. dissertation, Institut Teknologi Nasional, 2020.

[9] T. Ambreen, A. Saleem, and C. W. Park, "Numerical analysis of the heat transfer and fluid flow characteristics of a nanofluid-cooled micropin-fin heat sink using the Eulerian-Lagrangian approach," *Powder Technol.*, vol. 345, pp. 509–520, 2019. https://doi.org/10.1016/j.powtec.2019.01.042

[10] Y. Lin, Z. F. Wang, C. Y. Jim, J. B. Li, J. S. Deng, and J. G. Liu, "Water as an urban heat sink: Blue infrastructure alleviates urban heat island effect in mega-city agglomeration," *J. Clean. Prod.*, vol. 262, p. 121411, 2020. https://doi.org/10.1016/j.jclepro.2020.121411

[11] S. Zeng and P. S. Lee, "Topology optimization of liquid-cooled microchannel heat sinks: An experimental and numerical study," *Int. J. Heat Mass Transf.*, vol. 142, p. 118401, 2019. https://doi.org/10.1016/j.ijheatmasstransfer.2019.07.051

[12] C. J. Ho, Y. W. Guo, T. F. Yang, S. Rashidi, and W. M. Yan, "Numerical study on forced convection of water-based suspensions of nanoencapsulated PCM particles/Al2O3 nanoparticles in a mini-channel heat sink," *Int. J. Heat Mass Transf.*, vol. 157, p. 119965, 2020. https://doi.org/10.1016/j.ijheatmasstransfer.2020.119965

[13] A. Muhammad, D. Selvakumar, and J. Wu, "Numerical investigation of laminar flow and heat transfer in a liquid metal cooled mini-channel heat sink," *Int. J. Heat Mass Transf.*, vol. 150, p. 119265, 2020. https://doi.org/10.1016/j.ijheatmasstransfer.2019.119265

[14] H. Liu and X. Wang, "Aeroservoelastic design of piezo-composite wings for gust load alleviation," *J. Fluids Struct.*, vol. 88, pp. 83–99, 2019. https://doi.org/10.1016/j.jfluidstructs.2019.04.010

[15] H. Waqas, M. Fida, D. Liu, U. Manzoor, M. Alghamdi, and T. Muhammad, "Heat transport of nanofluid flow through a porous channel with thermal radiation effects," *Int. Commun. Heat Mass Transf.*, vol. 138, p. 106376, 2022. https://doi.org/10.1016/j.icheatmasstransfer.2022.106376

[16] Y. K. Wang, Y. G. Yin, and F. Cao, "Comprehensive evaluation of the transcritical CO2 ejector-expansion heat pump water heater," *Int. J. Refrig.*, vol. 145, pp. 276–289, 2023. https://doi.org/10.1016/j.ijrefrig.2022.09.008

[17] W. M. A. A. Japar, N. A. C. Sidik, R. Saidur, Y. Asako, and S. N. A. Yusof, "A review of passive methods in microchannel heat sink application through advanced geometric structure and nanofluids: Current advancements and challenges," *Nanotechnol. Rev.*, vol. 9, no. 1, pp. 1192–1216, 2020. https://doi.org/10.1515/ntrev-2020-0094

[18] A. M. A. Soliman, H. Hassan, and S. Ookawara, "An experimental study of the performance of the solar cell with heat sink cooling system," *Energy Procedia*, vol. 162, pp. 127–135, 2019. https://doi.org/10.1016/j.egypro.2019.04.014

[19] S. Wiriyasart and P. Naphon, "Liquid impingement cooling of cold plate heat sink with different fin configurations: High heat flux applications," *Int. J. Heat Mass Transf.*, vol. 140, pp. 281–292, 2019. https://doi.org/10.1016/j.ijheatmasstransfer.2019.06.020

[20] H. Li, X. H. Ding, D. Jing, M. Xiong, and F. Z. Meng, "Experimental and numerical investigation of liquid-cooled heat sinks designed by topology optimization," *Int. J. Therm. Sci.*, vol. 146, p. 106065, 2019. https://doi.org/10.1016/j.ijthermalsci.2019.106065

[21] J. W. Liu, Y. Zhang, D. B. Zhang, S. F. Jiao, Z. F. Zhang, and Z. H. Zhou, "Model development and performance evaluation of thermoelectric generator with radiative cooling heat sink," *Energy Convers. Manag.*, vol. 216, p. 112923, 2020. https://doi.org/10.1016/j.enconman.2020.112923

[22] S. Sun, P. Liebersbach, and X. Qian, "3D topology optimization of heat sinks for liquid cooling," *Appl. Therm. Eng.*, vol. 178, p. 115540, 2020. https://doi.org/10.1016/j.applthermaleng.2020.115540

[23] J. Wang, Y. P. Xu, R. Qahiti, M. Jafaryar, M. A. Alazwari, N. H. Abu-Hamdeh, A. Issakhov, and M. M. Selim, "Simulation of hybrid nanofluid flow within a microchannel heat sink considering porous media analyzing CPU stability," *J. Pet. Sci. Eng.*, vol. 208, p. 109734, 2022. https://doi.org/10.1016/j.petrol.2021.109734

[24] S. E. Ghasemi, A. A. Ranjbar, and M. J. Hosseini, "Experimental and numerical investigation of circular minichannel heat sinks with various hydraulic diameter for electronic cooling application," *Microelectron. Reliab.*, vol. 73, pp. 97–105, 2017. https://doi.org/10.1016/j.microrel.2017.04.028